NUMERICAL SIMULATION OF FRICTION STIR BUTT WELDING PROCESSES FOR AZ91 MAGNESIUM ALLOY

K. Senthil Kumar[1], M. Sivasangari[2], V. Rubesh Raj[3], L. Nirmal Raj[4]

[1] *Assistant Professor, MAR College of Engg & Technology, Viralimalai, India*
[2] *PG Student, DSEC, Coimbatore, India*
[3] *PG Student, Karpagam University, Coimbatore, India*
[4] *PG Student, PRIST University, Tanjore, India*

Abstract

Friction Stir Welding (FSW) is a solid state welding process. In particular, it can be used to join high-strength aerospace magnesium and other metallic alloys that are hard to weld by conventional fusion welding. It was performed on 4 mm thickness AZ91 Magnesium alloy. Magnesium alloy have more advantage than aluminum such as light weight, softer, tendency to bend easily, cost effective in terms of energy requirements so magnesium alloy has selected in this FSW technique. In friction stir welding (FSW), a momentous residual stress is present in weld due to complex nature of fixturing system compared to fusion welding. These residual stresses can affect properties of welded components during service. Therefore, for estimating magnitude of welding residual stresses and their nature of distribution along with thermal history, a three dimensional non- linear thermo-mechanical finite element (NLTMFE) model using ABAQUS/ CAE package was developed for butt welded magnesium alloy AZ91.

The objective of this work is to predict the temperature distribution in both materials and evaluate the mechanical properties during the friction stir welding on magnesium alloy.

Keywords: Fsw, Nltmfe, Abaqus, Cae, Az91.

---***---

1. INTRODUCTION

Friction stir welding (FSW) is a new, solid-state welding technique, which was invented by The Welding Institute (TWI) in 1991[1]. It has enabled us to long butt-weld Al alloys, which are often difficult to be fusion welded without void, cracking, or distortion. Basically, the detail of FSW process is that a non-consumable tool with a specially designed rotating pin is entered into abutting edges of a sheet or plate to be welded. Once entered, the rotating tool produces frictional heat and plastic deformation in the specimen. The tool is then translated along the joint to complete the joining process [1].

The recent studies, however, have restricted to Al alloys so that a few data have been published about FSW of Mg alloys and other materials. Mg alloys are potential candidate to replace Al alloys in many structural applications due to some of their unique properties. Mg alloys have a low density, high strength-to-weight ratio and good castability.

Magnesium is one of the most abundant elements in the earth's surface, with virtually inexhaustible supplies in the oceans. Over recent years the industrial output of magnesium alloys has been rising by almost 20% per annum, which is faster than that of any other metal [3]. The increased use of aluminum and magnesium alloys are of great interest to the automotive industry, with the goal of reducing the weight of road vehicles to make them more fuel efficient or to increase the vehicle specification without adversely affecting its fuel efficiency. In recent years there has been a renewed interest in the use of magnesium parts for body components, many of which have made by pressure die casting. These have limited ductility, contain gas occlusions, and are frequently difficult to weld satisfactorily by fusion welding techniques. With the major proportion of magnesium alloys being made by casting there has not previously been an extensive need for improved weldability to be developed [2].

2. EXPERIMENTAL WORK

The plates of AZ91 magnesium alloy were machined to the required dimensions (90 mm x 30 mm x 4 mm). Square butt joint configuration was prepared to fabricate the joints. The plates to be jointed were mechanically and chemically cleaned by acetone before welding to eliminate surface contamination. The direction of welding was normal to the rolling direction to the base metal. High-speed steel tool was used for welding AZ91 magnesium alloy having the shoulder diameter of

20mm. The tool had a pin height of 3 mm and a 4 mm pin diameter.

The vertical milling machine has been used to perform the welding process the automatic operated conditioned type of vertical milling machine selected for doing the welding process. The ordinary fixture of milling machine cannot be used for this process. So, the fixture designing is very important role in the welding process. The fixture has been designed for the dimensions of the work pieces. The work pieces clamped to the fixture. The fixture placed in the work table. The fixture is used for arrest the movement of the work piece. The tool is placed in the tool holder by using collect of 25mm diameter. The vertical milling machine is checked for the conditions and also the parameters for the welding process. The welding process is having three phases like Plunging, Stirring, and Retracting. The welding process can be done by the vertical milling machine. The tool slowly plunged to the work pieces, the required feed rate is given to the machine then the weld can be performed. The welding process is performed at various parameters.

The rolled plates of magnesium alloy were machined to the required dimensions (100 mm x 100 mm x 5 mm). Square butt joint configuration was prepared to fabricate the joints. The plates to be joined were mechanically and chemically cleaned by acetone before welding to eliminate surface contamination. The direction of welding was normal to the rolling direction. Necessary care was taken to avoid joint distortion and the joints were made by securing the base metal. A non-consumable, rotating tool made of high carbon steel was used to fabricate FSW joints.

The plates are prepared to measure the temperature at 8 points using thermocouples. On each plate, four 6mm diameter holes were drilled on one side of the plate.

Type K thermocouples of 5 mm diameter are subsequently inserted into the holes and glued so that the thermocouple ends are in intimate contact with the workpiece. The locations of thermocouples in the workpiece are shown in figure 13.

The welding was carried out at room temperature. In some cases intensive cooling of the surface of the sheets, which were earlier cooled down to about 259 K (-14oC), was implemented. The cooling was performed by pouring granulated dry ice (CO_2) on the surface of the sheets being joined. The samples were investigated in the after-welding state (the samples stored at the temperature of 243K (-30oC). The joint performance was determined by conducting optical microscopy, micro hardness measurements and mechanical testing (e.g. Tensile and bend tests)

The high speed steel raw material has been taken the tool materials. The tool was designed based on the chuck of the radial drilling machine. Then the tool was heat treatment applied to increase the hardness. Improvements in tool design

have been shown to cause substantial improvements in productivity and quality. TWI has developed tools specifically designed to increase the depth of penetration and so increase the plate thickness that can be successfully welded.

3. TOOL DESIGN

The design of the tool is a critical factor as a good tool can improve both the quality of the weld and the maximum possible welding speed.
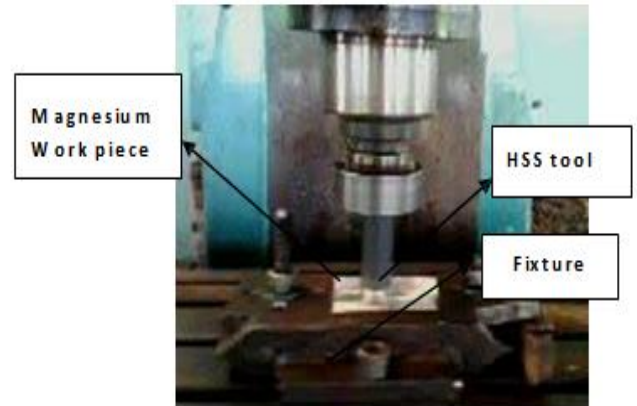
Fig: 3.1.4 Friction stir welding process in stirring stage.
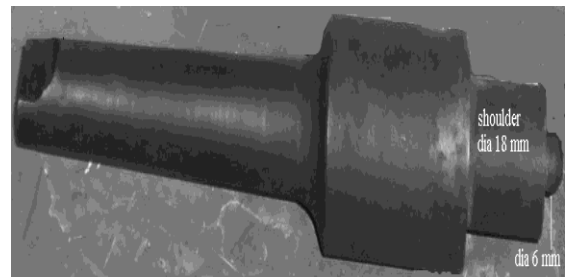
3.2.1 Tool design

3.3.1. Fixture set-up

3.3.2 Temperature controller

It is desirable that the tool material is sufficiently strong, tough and hard wearing, at the welding temperature. Further it should have a good oxidation resistance and a low thermal conductivity to minimize heat loss and thermal damage to the machinery further up the drive train. Hot-worked tool steel such as AISI H13 has proven perfectly acceptable for welding aluminium alloys within thickness ranges of 0.5 – 50 mm but more advanced tool materials are necessary for more demanding applications such as highly abrasive or higher melting point materials such as steel or titanium.

4. ASSUMPTIONS IN NUMERICAL ANALYSIS

The following assumptions are made in developing the model:

- The heat generation is due to friction only.
- Heat generated during penetration and extraction is not considered.
- The coefficient of friction is considered as constant.
  - Material properties are uniform.
  - Heat transfer by radiation is negligible.

The important process characteristics which are required to be considered for the purpose of modeling are as follows:

      a) Moving heat source;
      b) Weld speed;
      c) Axial load and
      d) Material properties

4.1 Nomenclature

    c - Specific heat, J/kg K
    ρ - Density, kg/m3
    h - Heat transfer coefficient, W/m^2 K
    k - Thermal conductivity, W/m K
    ω - Angular speed of tool, r/s

Fn - Normal force, N Q - Heat generated, J
Ri - Radius of the pin, mm
Ro - Radius of the shoulder.

4.2 Governing Equation

The general three dimensional partial differential equation of heat conduction in solid can be represented by

$$\delta(\rho ct)/\delta t = \delta/\delta t(K_X \, \delta T/\delta x) + \delta/\delta t(K_Y \, \delta T/\delta y) + \delta/\delta t(K_Z \, \delta T/\delta z)$$

This differential equation with its associated boundary conditions can be solved using various numerical procedures such as finite difference, finite element and control Volume methods. In the present work, the temperature distribution during welding is modeled using finite element method. [7]

Where
    ρ is the density
    c is the specific heat T is the temperature t is the time taken
    K is the conductivity in the x, y, z direction.

The two plates that are to be welded are identical. At the centerline of the work piece, the temperature gradient in the transverse direction, i.e., $\delta T/ \delta y$, equals zero due to the symmetrical requirement. The initial temperature of the work piece is assumed to be atmospheric temperature 296 K. The heat transfer during penetration and pulling out period is not considered.

The heat source in FSW is considered to be friction between the tool shoulder and work piece surface. The local heat generated over the interface of the contact surface can be calculated by the following expression

$$Q = 1/2 \; [\mu \, F_n \, (R_i + R_0) \, \omega]$$

The coefficient of friction μ varies with temperature. But in this model an effective coefficient of friction of 0.4 is considered. F_n is the axial force, ω is the axial force; R_i is the radius of the tool pin, R_O is the radius of tool shoulder and Q is the heat generated.

4.3 Modeling and Solution

In this investigation a three- dimensional symmetric model is developed, to predict the temperature and the stress distribution in the work piece by using the friction stir welding using Abaqus/ CAE finite element package [7]. The work piece is extruded rectangular plate of dimension 100 x50 x 6 mm and the tool is revolved cylindrical tool of circular cross section with the tool pin diameter of 6mm as shown in fig 4.3.1 and fig4.3.2.
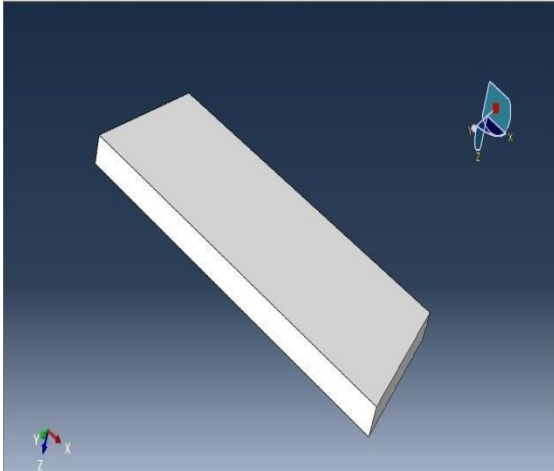
Fig 4.3.1 modeling of work piece

Fig 4.3.2 Tool

The modeled parts are assembled and is shown in fig 4.3.3 .The mesh of the work piece and that of tool comes under the mesh family of coupled temperature-Displacement of tetrahedron elements, the mesh is C3D4T a 4 Node thermally coupled tetrahedron, linear displacement and temperature is used and the mesh of the assembly is shown in fig 4.3.4. The boundary conditions are to be applied to the model. The work piece shouldn't move hence it is to be enraptured and in the tool displacement, rotation,   Velocity and angular velocity are to be applied.

In the tool a force of 3000 N is applied and in the work piece the temperature is applied; after applying all the boundary conditions we have to submit the model for analysis and the results are taken. The boundary condition and load applied are shown in fig 4.3.5.

Fig 4.3.3 Assembly of the tool and work piece
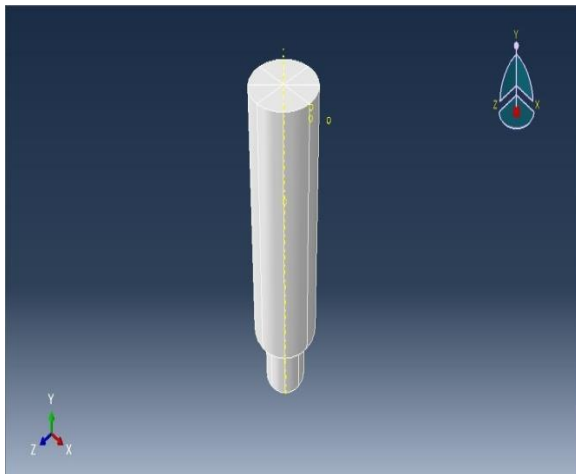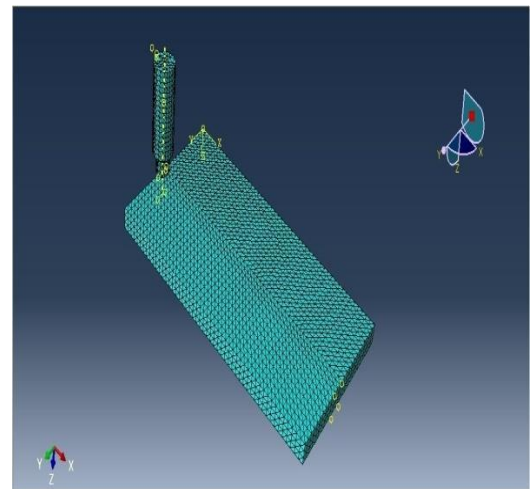
Fig 4.3.4 Mesh of the assembly
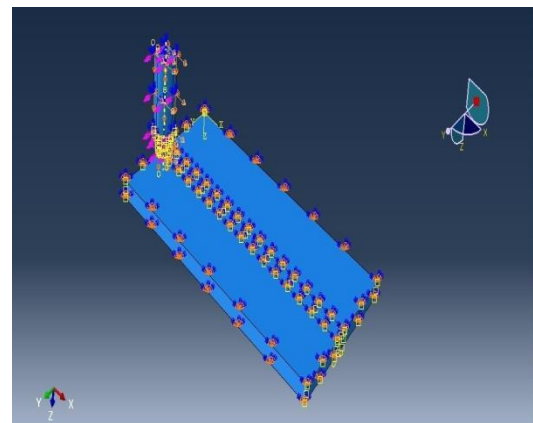
Fig 4.3.5 Boundary conditions applied in the assembly

In the boundary condition all the sides of work piece is enraptured i.e. neither rotation nor movement of the work

piece. In abaqus before applying load we have to create steps as to which the movement of the tool goes smoothly. In the steps option we are choosing the coupled temperature displacement. In the step we are choosing Steady state response and choosing the option *nlgeom* option to include the non linear effects of large deformation and displacements so as to provide good results [8].

5. RESULTS AND DISCUSSIONS

5.1 Residual Stress:
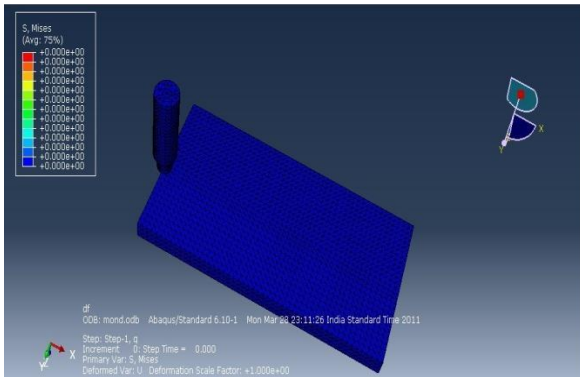
Fig 5.1.1 Residual stress at the step1
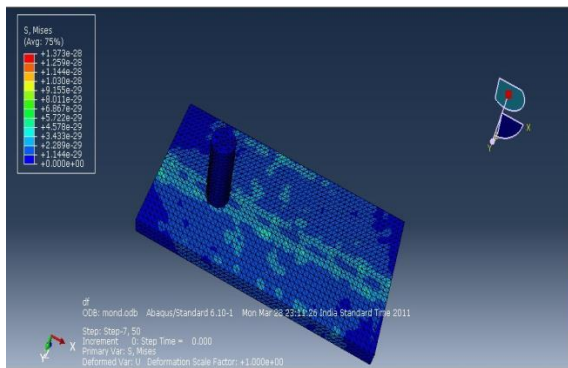
Fig 5.1.2 Residual stress at step-7
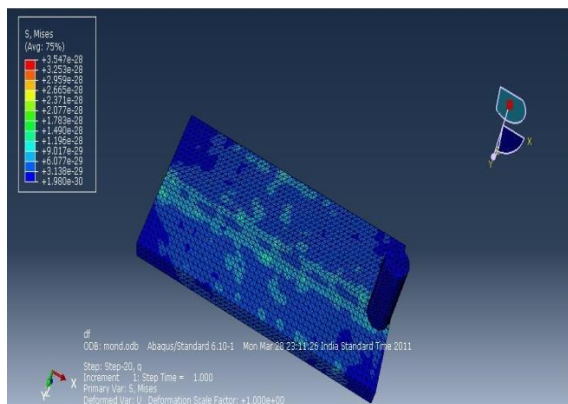
Fig 5.1.3 Residual stress at step 21

From the residual stress analysis which is the von mises stress the maximum stress in the work piece is found out to be $6.077e\text{-}29$ N/mm^2 and the distribution of residual stress in work piece is highly uneven in nature and the residual stress is maximum along the weld path compared to the base metal. This uneven nature of residual stress is due to the clamping of work piece in a fixture which restricts all movement of the work piece [9].

5.2 Temperature Distribution in Work Piece:
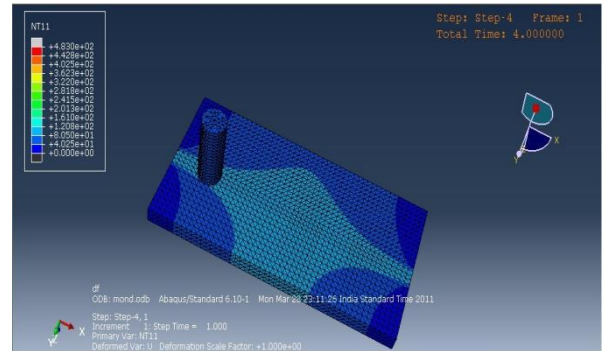
Fig 5.2.1 Temperature distribution at step 4
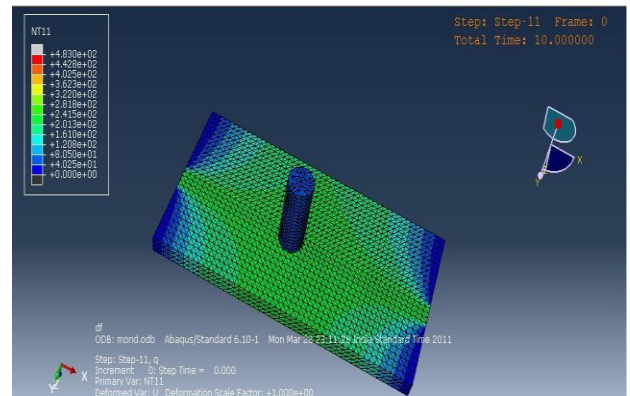
Fig 5.2.2 Temperature distribution at step 11
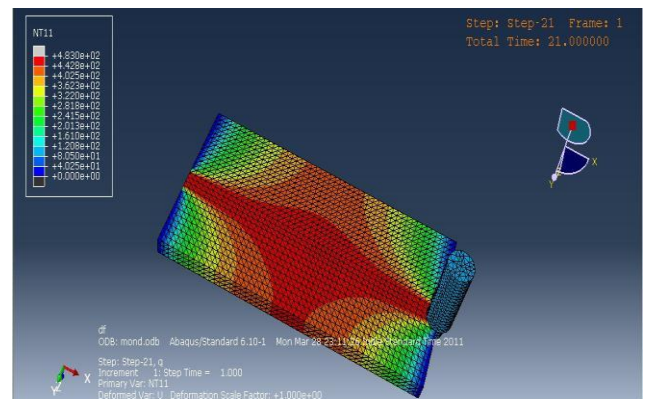
Fig 5.2.3 temperature distribution at step 21

The maximum temperature attained by the process is 483°C, also the maximum temperature distribution is found in the advancing side of the weld and along the weld path.

5.3 Pressure Distribution
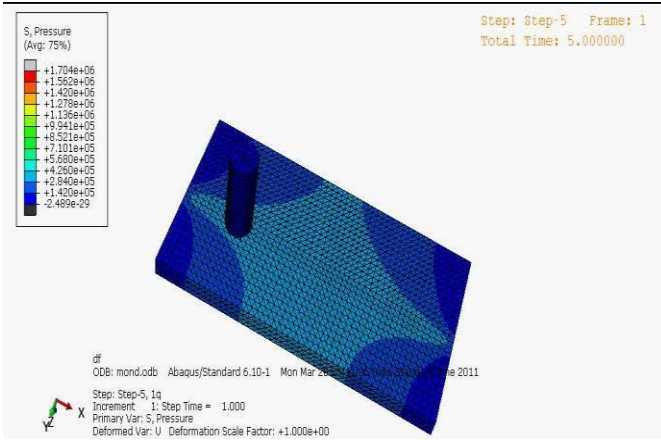
Fig 5.3.1 Pressure at step 5
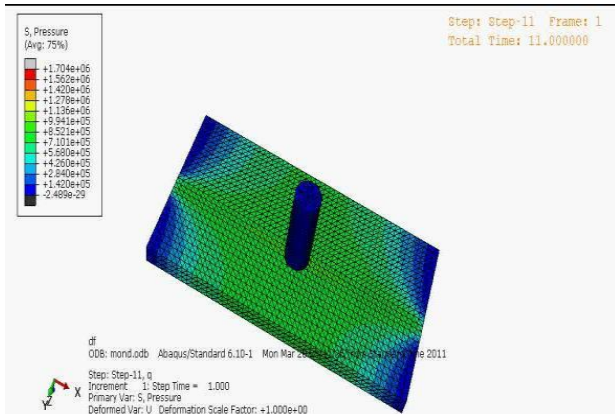
Fig 5.3.2 pressure at step 11
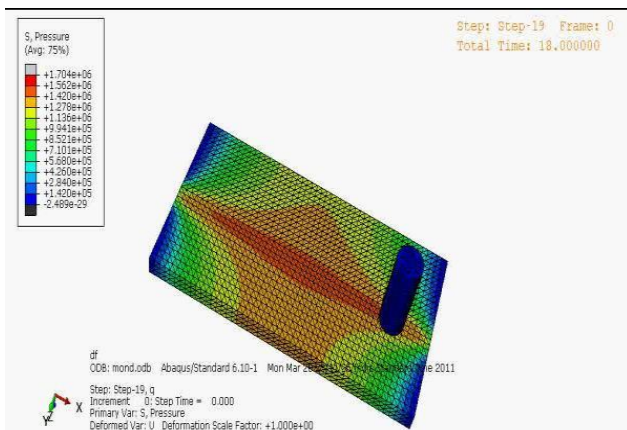
Fig 5.3.3 pressure at step 19

The pressure is maximum along the weld path in the midpoint of the work piece of the order 1.704e+06 N/mm^{2} and along the advancing and retreating side of the work piece the pressure is of the order of

1.278e+06 N/mm^{2}

5.4 Analysis of Various Parameters
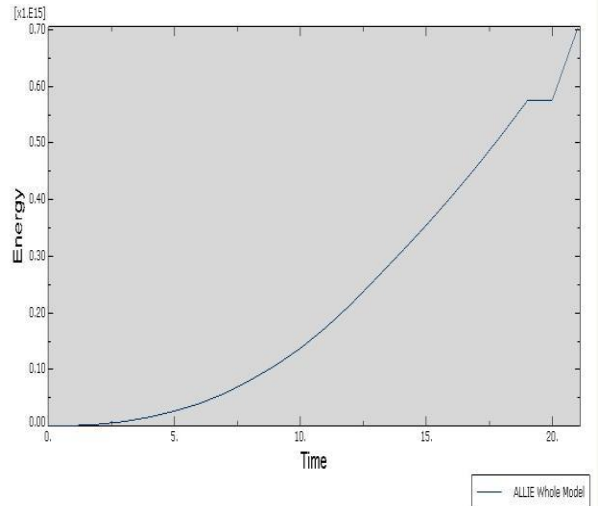
Fig 5.4.1 Graph: Internal Energy Vs Time

The internal energy of the work piece with respect to time is plotted. The energy increases gradually up to time of 18seconds and for 2 seconds the internal energy is the same in the work piece which is of the order of 0.60x1E15 and the maximum achieved is 0.70x1E15
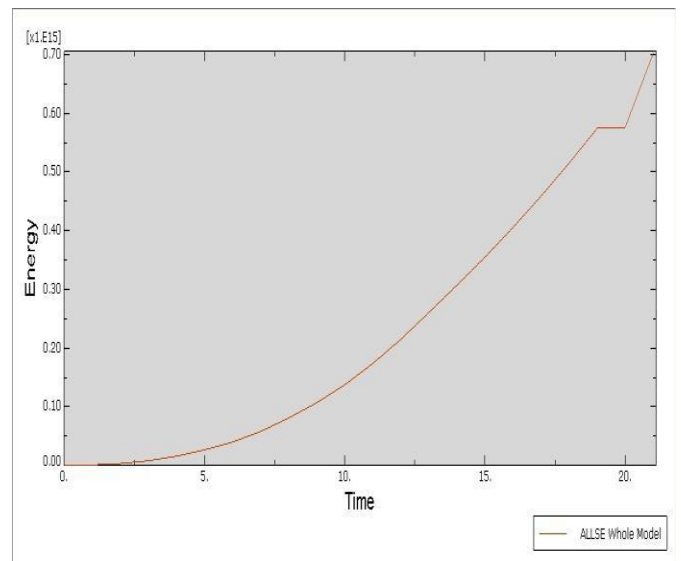
Fig 5.4.2 Graph: Strain energy Vs Time

In this graph the strain energy gradually increases and has a maximum of 0.70x1E15 also the strain energy is the same at 0.58x1E15 from the time 18th Second to 30th second.
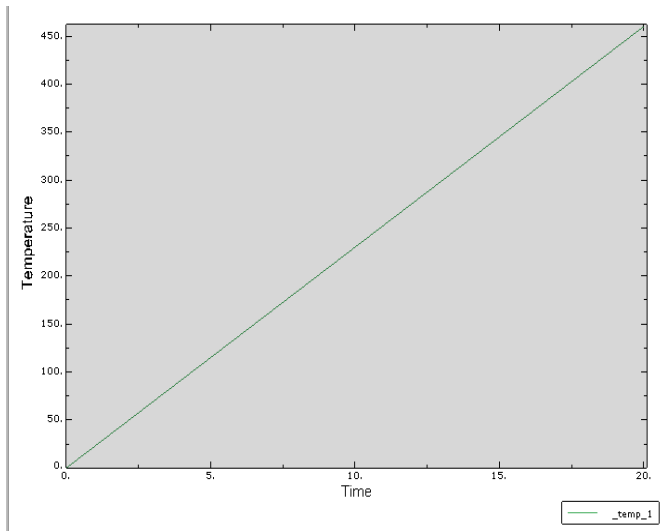
Fig 5.4.3 Graph: Temperature Vs Time

In the temperature vs. time graph the temperature in the work piece increases linearly with respect to time and is within $500^{o}C$
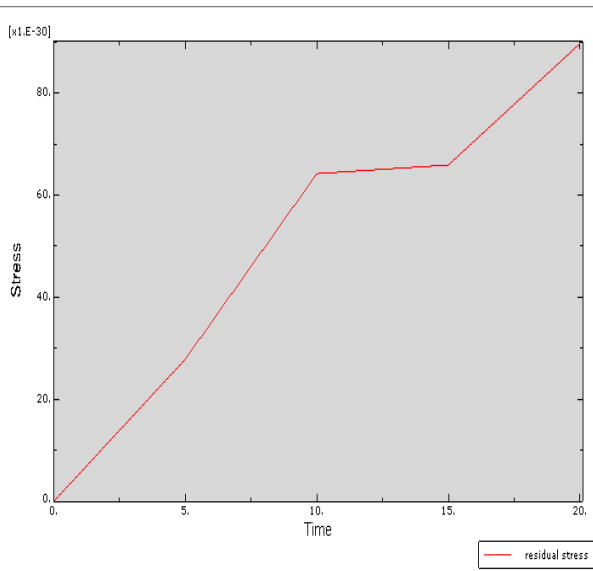
Fig 5.4.4 Graph: Residual stress Vs Time

The graph is plotted between residual stress and time, in this the residual stress increases up to 9 seconds and it becomes stable from 10 to 15 seconds and then again increases. The residual stress at the stable region is 60x1E-30
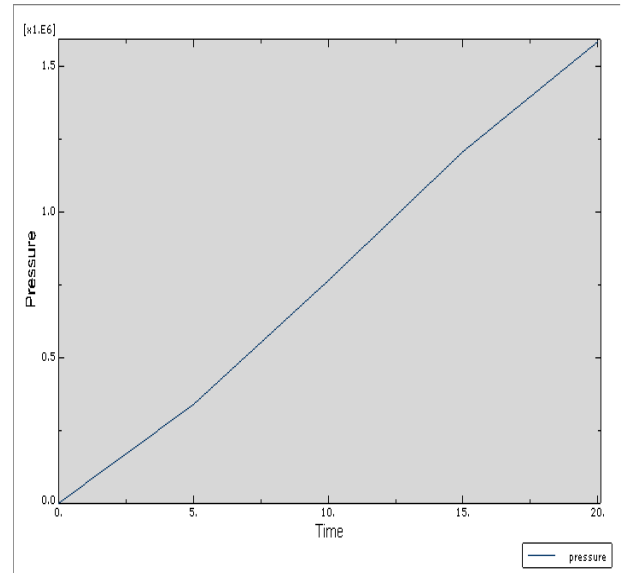
Fig 5.4.5 Graph: Pressure Vs Time

In this graph pressure and time is plotted. The pressure increases linearly with respect to time and the maximum pressure applied in the work piece is 1.5x1E6
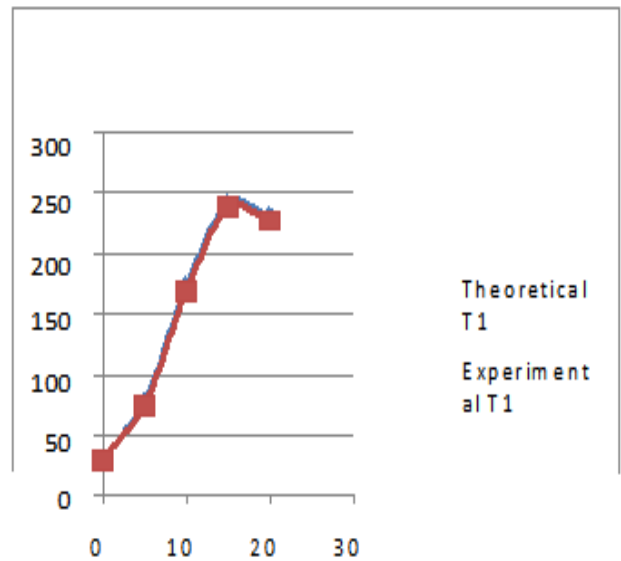
Fig 5.4.6 Temperature T_1 Vs Time

From the thermocouple T_1 which is measured at a distance of 10 mm and 5 mm in the advancing side from the weld path and the temperature increases gradually and then decreases and is correlated with that of theoretical values obtained through ABAQUS® and the values are nearer to the experimental values.
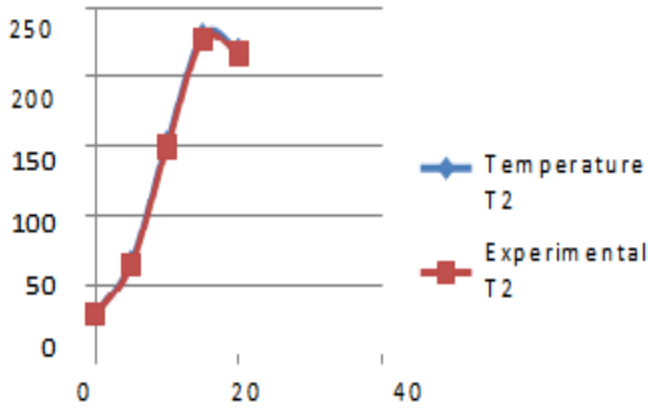
Fig 5.4.7 Temperature T_2 Vs time

From the thermocouple T_2 which is measured at a distance of 10 mm and 5 mm in the retreating side from the weld path and the temperature increases gradually and then decreases and is correlated with that of theoretical values obtained through ABAQUS$^®$ and the values are nearer to the experimental values.
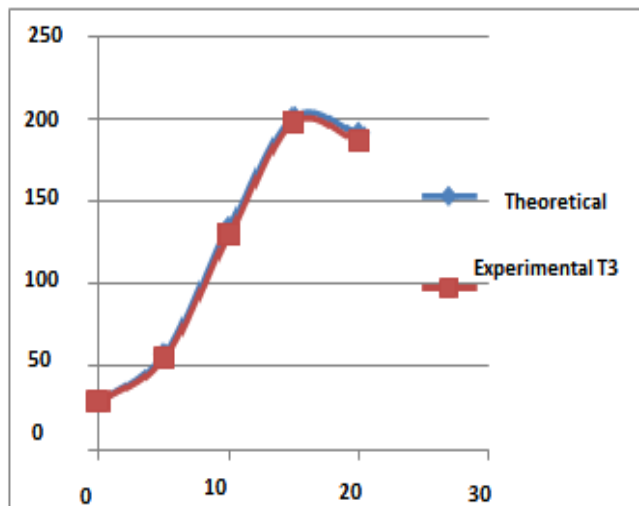
Fig 5.4.8 Temperature T_3 Vs Time

From the thermocouple T_3 which is measured at a distance of 75 mm and 5 mm in the retreating side from the weld path and the temperature increases gradually and then theoretical values obtained through experimental values.
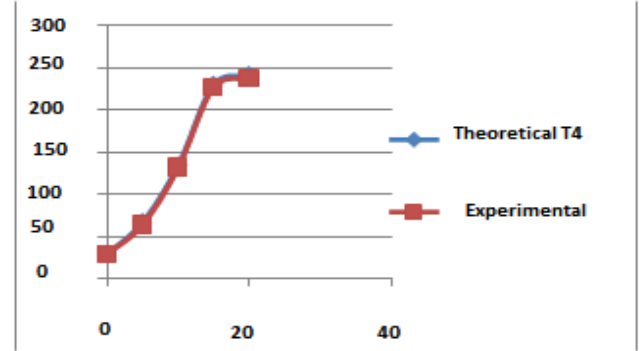
Fig 5.4.9 Temperature T4 Vs Time

From the thermocouple T_4 which is measured at a distance of 75 mm and 5 mm in the advancing side from the weld path and the temperature increases gradually and then decreases and is correlated with that of theoretical values obtained through ABAQUS$^®$ and the values are nearer to the experimental values.
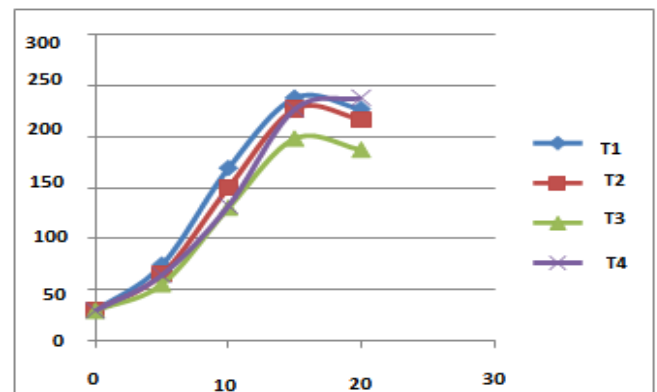
Fig 5.4.9 Experimental
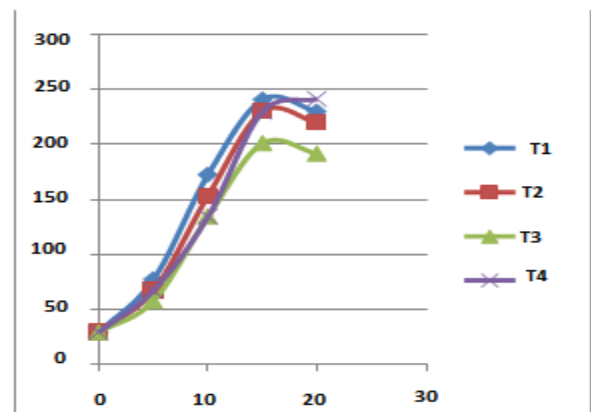
Fig 5.4.10 Theoretical

6. CONCLUSIONS

Numerical analysis can be successfully applied to the modeling of stress and temperature distribution in friction stir welding. The results obtained from this investigation are as follows:

- The measurement of temperature in the weld path is very rare; hence the temperature is measured by means of k type thermocouple at four places in the base metal in the advancing and retreating side of the weld.

- The experimental values are correlated with that of the theoretical values obtained and found that the theoretical values are closer to the experimental values.

- The temperature obtained by using numerical analysis along the weld path is approximate to the temperature in the real time friction stir welding.

- The simulation is used to check the correct parameters and thereby saving the time.

REFERENCES

[1]   Thomas WM, Nicholas ED, Needham JC, Church MG, Templesmith P, Dawes CJ Frictions stir welding. International Patent Application no PCT/GB92102203 and Great Britain Patent Application no.9125978.8; 1991

[2]   Friction Stir Lap Welding of Magnesium Alloy and Zinc-Coated Steel- Y. C. Chen* and K. Nakata

[3]   Benjamin Landkof, "Magnesium Flammability Test", "Mg Broad Horizons" Conference, St. Petersburg, 6th – 8th of June

[4]   2007

[5]   Peel M, Steuwer A, Preuss M, Withers PJ. Microstructure, mechanical properties and residual stresses as a function of welding speed in aluminium AA5083 friction stir welds. Acta Mater 2003;51(16):4791–801.

[6]   Mechanical Properties of 6013-T6 Aluminium Alloy Friction Stir Welded Plate- Haşim KAFALI*, Nuran AY.

[7]   YUH J Chao, X.Qi, W.Tang - Heat transfer in friction stir welding- Experimental and numerical studies.

[8]   N. Rajamanikam, V.Balusamy - Numerical Simulation of Transient Temperature in Friction Stir Welding of Aluminum Alloy 2014 -T6.

[9]   Diego Santiago et al - 3D Modeling of Material Flow and Temperature in Friction Stir Welding

[10] Zhao zhang and Hongwu zhang - The Simulation of Residual Stresses In Friction Stir welds.

[11] N. Rajamanickam, V. Balusamy et al - Numerical simulation of thermal history and residual stresses in friction stir welding of Al 2014-T6

[12] Friction stir welding of Magnesium Alloys by Dr Richard Johnson, Dr Philip Threadgill.

[13] Won-bae Lee et al - Microstructure and Mechanical properties of Friction stir welded AZ31Magnesium alloy

[14] Manthan malde Thermo mechanical modeling and Optimization of Friction Stir Welding.

[15] Ronald P. Cooper et al Friction stir welding of Magnesium AM60 alloy.

[16] Yan yong et al. Dissimilar frictions stir welding between 5052 aluminum alloy and AZ31 magnesium alloy.